GEOLOGICA CARPATHICA, APRIL 2011, 62, 2, 155–169 doi: 10.2478/v10096-011-0013-z

Integrated high-resolution stratigraphy of a Middle to Late Miocene sedimentary sequence in the central part of the Vienna Basin

WIESKE E. PAULISSEN[1], STEFAN M. LUTHI[1], PATRICK GRUNERT[2], STJEPAN ĆORIĆ[3] and MATHIAS HARZHAUSER[4]

[1]Department of Geotechnology, Delft University of Technology, Stevinweg 1, 2628 CN Delft, The Netherlands; w.e.paulissen@tudelft.nl; s.m.luthi@tudelft.nl
[2]Institute for Earth Sciences, University of Graz, Heinrichstrasse 26, A-8010 Graz, Austria; patrick.grunert@uni-graz.at
[3]Geological Survey of Austria, Neulinggasse 38, A-1030 Vienna, Austria; stjepan.coric@geologie.ac.at
[4]Natural History Museum Vienna, Burgring 7, A-1010 Vienna, Austria; mathias.harzhauser@nhm-wien.ac.at

(Manuscript received April 16, 2010; accepted in revised form October 11, 2010)

Abstract: In order to determine the relative contributions of tectonics and eustasy to the sedimentary infill of the Vienna Basin a high-resolution stratigraphic record of a Middle to Late Miocene sedimentary sequence was established for a well (Spannberg-21) in the central part of the Vienna Basin. The well is located on an intrabasinal high, the Spannberg Ridge, a location that is relatively protected from local depocentre shifts. Downhole magnetostratigraphic measurements and biostratigraphical analysis form the basis for the chronostratigraphic framework. Temporal gaps in the sedimentary sequence were quantified from seismic data, well correlations and high-resolution electrical borehole images. Stratigraphic control with this integrated approach was good in the Sarmatian and Pannonian, but difficult in the Badenian. The resulting sedimentation rates show an increase towards the Upper Sarmatian from 0.43 m/kyr to > 1.2 m/kyr, followed by a decrease to relatively constant values around 0.3 m/kyr in the Pannonian. The sequence reflects the creation of accommodation space during the pull-apart phase of the basin and the subsequent slowing of the tectonic activity. The retreat of the Paratethys from the North Alpine Foreland Basin during the Early Sarmatian temporarily increased the influx of coarser-grained sediment, but eventually the basin acted mostly as a by-pass zone of sediment towards the Pannonian Basin. At a finer scale, the sequence exhibits correlations with global eustasy indicators, notably during the Sarmatian, the time of greatest basin subsidence and full connectivity with the Paratethyan system. In the Pannonian the eustatic signals become weaker due to an increased isolation of the Vienna Basin from Lake Pannon.

Key words: Miocene, Vienna Basin, high-resolution stratigraphy, biostratigraphy, downhole magnetostratigraphy, global sea-level.

Introduction

The history of the epicontinental Central Paratethys is characterized by a highly dynamic paleogeography. In an environment of changing sea-ways and land-bridges, and with intermittent isolation of the Paratethys from the oceanic realm, a mainly endemic flora and fauna developed. The regional stratigraphy is based on this unique fossil record, but the endemic character of the biota causes great difficulties in correlating the Central Paratethyan records to the Mediterranean and the global stratigraphic records (Piller et al. 2007). Magnetostratigraphic studies from the Central Paratethyan region are limited primarily because of variable outcrop conditions and the lack of long, continuous sections (Scholger & Stingl 2004; Magyar et al. 2007). Therefore, correlation of the regional stratigraphy to the global stages is often based on sequence stratigraphic studies using seismic and well data, with ages assigned through correlation to 3rd order sea-level cycles (Kreutzer 1986; Weissenbäck 1996; Harzhauser et al. 2004; Kováč et al. 2004; Strauss et al. 2006). Recently, Lirer et al. (2009) proposed a correlation of an orbitally tuned Middle to Late Miocene sedimentary record from the Vienna Basin to an astronomically calibrated Mediterranean deep marine record. However, a good consensus has not yet been reached on the exact timing of the stratigraphic stage boundaries for the Central Paratethys and hence for the timing of the sedimentary infill of the Vienna Basin.

The Vienna Basin is a suitable area for a high-resolution stratigraphic study since it went through a phase of rapid tectonic subsidence during the Middle to Late Miocene (Lankreijer et al. 1995), resulting in a thick sedimentary sequence that provides a detailed temporal record. Accurate age dating of the sedimentary infill of the Vienna Basin could thus assist in evaluating the relative contributions of tectonics, eustasy and other factors. The purpose of the present study is therefore to establish a high-resolution stratigraphic analysis of the sedimentary sequence penetrated by a well in the central part of the Vienna Basin. With the resulting temporal record, sedimentation rates of the sequence can then be accurately determined, providing detailed insights into the sedimentary and tectonic evolution of the basin infill of the Vienna Basin on a local and conceivably also on a regional scale.

The approach of this study relies on combining seismic data with high-resolution well data, thereby integrating different

stratigraphic scales. The well is an actual production well in which additional measurements have been performed specifically for the purpose of this study. It traverses the Middle to Late Miocene sequence in a relatively central part of the basin, away from shifting depocentres at the basin margins and in a position where few stratigraphic unconformities are expected. Aside from seismic, the acquired data include standard well logs (in logging-while-drilling mode) as well as cuttings. The data specifically acquired for this study include a magnetostratigraphic record with a novel wireline logging tool that provides a continuous record of the polarities of the remanent magnetization of the sedimentary sequences traversed by the borehole. Because the Miocene contains a large number of normal and reverse polarities this logging tool provides the opportunity to attain absolute age dating at a higher resolution than can be achieved with biostratigraphical analysis alone. Another log run specifically for this study is the Formation MicroImager (FMI, Mark of Schlumberger) which provides high-resolution borehole images that are used to characterize bedding types and, in combination with seismic data, to identify unconformities and faults in order to further refine the time lines.

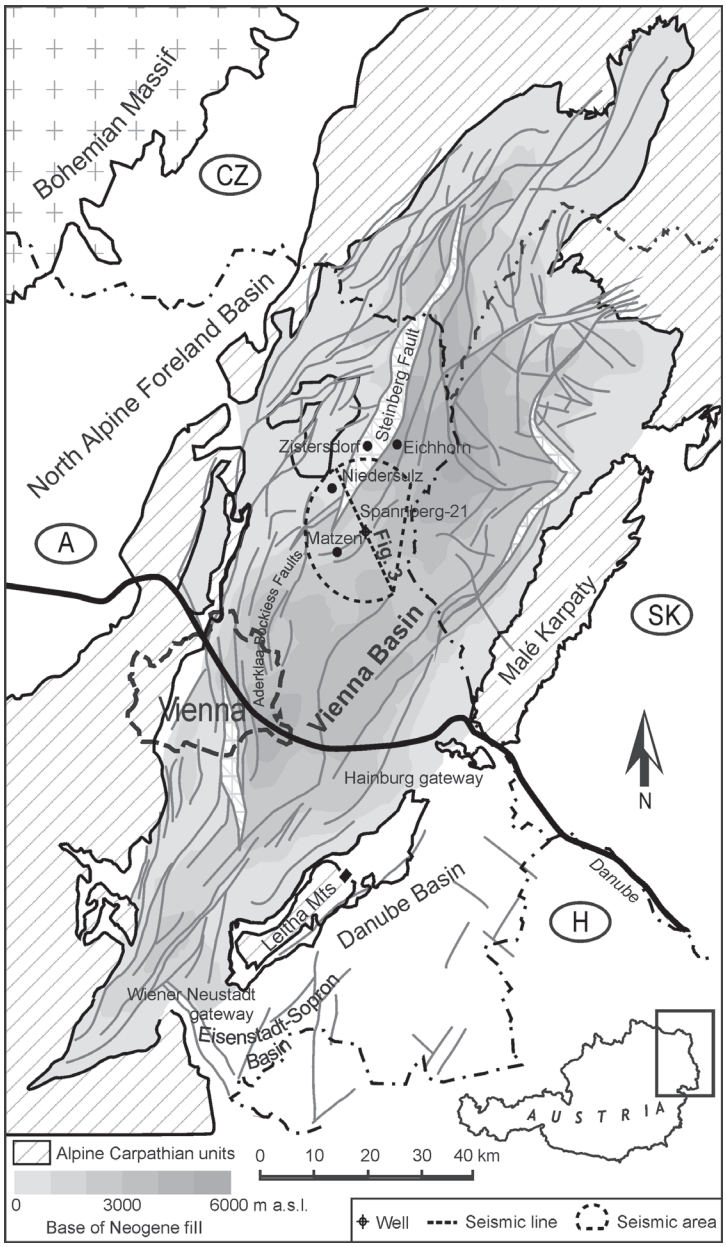

Fig. 1. Structural setting of the Vienna Basin with the main structural units in the Eastern Alpine-Carpathian region (modified after Decker et al. 2005 and Harzhauser et al. 2004). The base of the Neogene infill in the Vienna Basin is indicated in grey-scale. The black dots indicate village locations associated to wells mentioned in the text. The area of the seismic lines is indicated with stippled lines.

Geological setting of the Vienna Basin

Location

The Vienna Basin forms the north-western part of the Pannonian basins complex system and is situated in the external zone of the Alpine-Carpathian thrust belt. It has two main depocentres (Kováč et al. 2004; Hinsch et al. 2005b) which were fed mainly by detritus from the Bohemian Massif, the North Alpine Foreland Basin and by the eroding and extending Alpine orogen.

Figure 1 shows the Vienna Basin spreading from the Czech and Slovak Republic in the North to NE Austria in the South. It is rhomboidal in shape with a SSW-NNE orientation and is 60 km in width and 200 km in length. During Middle Miocene times the Vienna Basin was a semi-closed basin and the connection with the Central Paratethys was restricted to the Wiener Neustadt gateway towards the Eisenstadt-Sopron Basin, and to the Hainburg gateway towards the Danube Basin (Fig. 1) (Harzhauser et al. 2004). To the northwest it is separated from the North Alpine Foreland Basin by external thrust sheets of the Alpine-Carpathian system. According to Kilényi & Šefara (1989) the Vienna Basin has a maximum Neogene infill of 5500 m.

Basin evolution

The evolution of the Vienna Basin can be subdivided into three distinctly different phases, each with its own geodynamic and sedimentary characteristics (Wessely 2000). The first phase started in the Early Miocene when the tectonic system of the Eastern Alps transformed from a N-S compression to eastward lateral extrusion along prominent transform faults (Ratschbacher et al. 1991; Peresson & Dekker 1997). The Vienna Basin formed on top of these thrust sheets as a piggyback basin in a NW-SE compressional system (Seifert 1992; Kováč et al. 1998b; Hölzel et al. 2010). During the Eggenburgian sedimentation took place in the northern part of the slowly subsiding basin, prograding southward during the Ottnangian and Early Karpatian and resulting in the dep-

osition of lacustrine to brackish-littoral sediments (Kováč et al. 2004) (Fig. 2).

The second phase started during the Late Karpatian when thrusting developed into lateral extrusion of the Western Capathians from the Eastern Alpine domain, with the basin undergoing a change into a pull-apart basin (Lankreijer et al. 1995; Decker & Peresson 1996; Seifert 1996; Kováč et al. 2004). Subsidence of the basin was dominated by NE-SW oriented left-lateral strike-slip faults during the Late Karpatian to the earliest Badenian on the eastern margin of the basin (Leitha Fault System) and from the Lower to Middle Badenian on the western margin of the basin (Schrattenberg and Bulhary Fault System) with the formation of grabens, half-grabens and uplifted blocks (Kováč et al. 2004). As a consequence of the change in tectonics an inversion took place at the Karpatian/Badenian boundary, leading to erosion of large volumes of Early Miocene deposits (Steininger & Wessely 2000). The main depocentre shifted southward, where a large deltaic system developed with fluvio-deltaic conditions in the south and a limnic-deltaic complex towards the centre (Aderklaa Formation). In the northern part of the basin, marine conditions with shaly sedimentation continued to prevail (Sauer et al. 1992).

The marine sedimentation in the Vienna Basin reached its maximum extent during the Badenian with fine-grained sedimentation in the basinal parts (Sauer et al. 1992; Weissenbäck 1996). In shallow coastal regions along the basin margins and on uplifts within the basin, coastal terraces and corallinacean shoals with scattered coral patch reefs formed (Leitha Limestone; Weissenbäck 1996; Riegl & Piller 2000). The Middle Miocene deltaic bodies were sourced from the western (paleo-Danube River) and northern margins (paleo-Morava River) of the basin. A drop in relative sea-level at the end of the Badenian is considered to be the cause of significant erosion of Badenian deposits across the basin (Kováč et al. 2004).

The NW-SE extension continued throughout the Sarmatian with a period of more rapid tectonic subsidence during the Early Sarmatian along the ENE-WSW sinistral strike-slips and NE-SW oriented normal faults (Wagreich & Schmid 2002; Kováč et al. 2004; Decker et al. 2005). The sedimentary conditions remained comparable to those of the Badenian except that the paleoenvironment switched from normal marine towards a stressed system with hyper- and hyposaline conditions and phases of eutrophication (Wessely 1988; Harzhauser & Piller 2004; Harzhauser & Kowalke 2004).

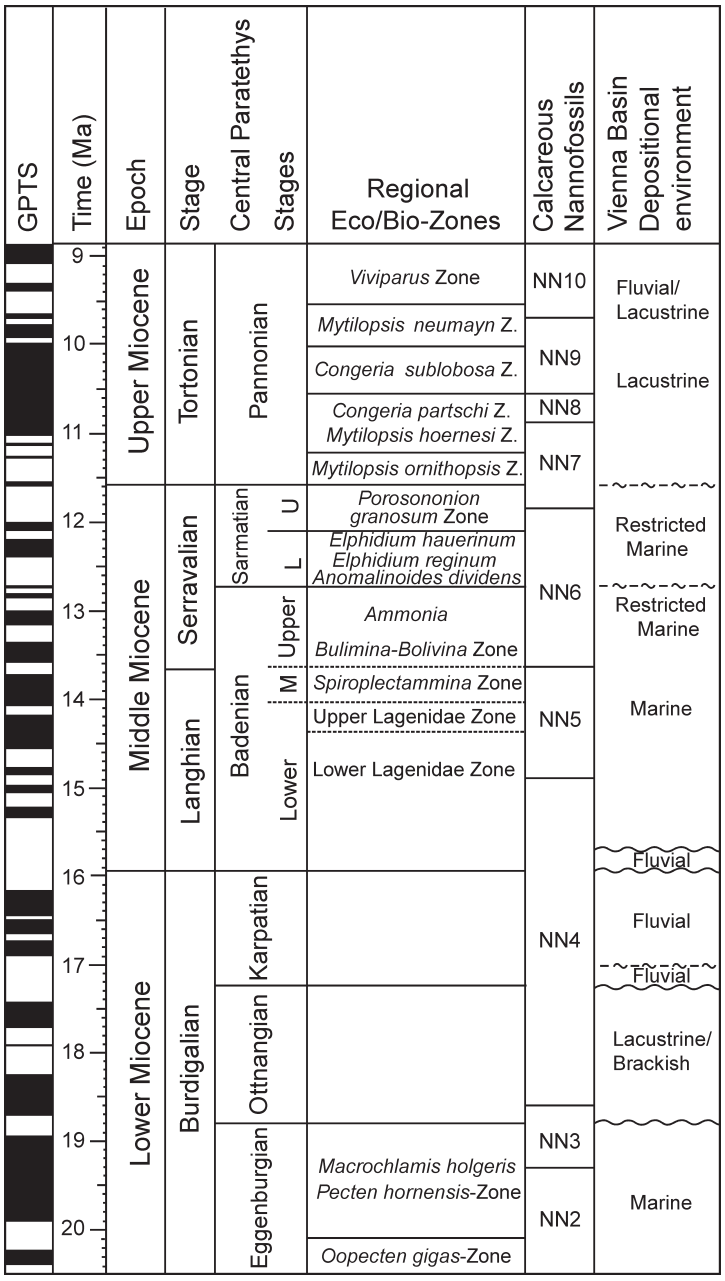

Fig. 2. Chronostratigraphic and biostratigraphic zonation as well as the general depositional environments of the Vienna Basin during the Miocene. Biozones are from Cicha et al. (1998) and the geomagnetic polarity timescale from Lourens et al. (2004). The main Central Paratethyan stage boundaries are according to Strauss et al. (2006) and the Sarmatian substage boundaries according to Harzhauser & Piller (2004).

Starting from the Pannonian the Central Paratethys developed into an alkaline lake system called Lake Pannon, an enclosed basin framed by the Alps, the Carpathians and the Dinarids (Steininger & Rögl 1985; Kázmér 1990; Magyar et al. 1999; Harzhauser & Mandic 2008). The transition from the Sarmatian to the Pannonian is characterized by a strong regression and erosion along the basin margins (Kreutzer & Hlavatý 1990; Kováč et al. 2004). The Vienna Basin was filled by deltas prograding from NW towards SE during the Early and Middle Pannonian (Seifert 1996), followed by fluvial deposits in the Late Pannonian. According to Decker & Peresson (1996) and Cloetingh & Lankreijer (2001) a change in the large-scale stress field caused the onset of the third phase of the Vienna Basin in the Late Pannonian with the regime changing into an E-W compressive stress field, resulting

in basin inversion and subsequently the termination of pull-apart kinematics (Decker et al. 2005).

Timing of the basin infill

The timing of the Vienna Basin infill phases is not accurately known because of a lack of reliable age data. A linkage to regional or global sequences has been attempted by various authors based on seismic stratigraphy and biostratigraphy (Rögl 1998; Harzhauser et al. 2004; Strauss et al. 2006). The period of interest in this study covers the Middle to Late Miocene, corresponding to the Central Paratethyan regional stages from the Lower Badenian to the Upper Pannonian (Fig. 2).

While the lower boundary of the Late Badenian is commonly assumed to correspond to the Langhian/Serravallian boundary at 13.65 Ma (Lourens et al. 2004; Piller et al. 2007; Kováč et al. 2007), there are uncertainties concerning the age of the Sarmatian. According to Harzhauser et al. (2004) it spans the entire 3rd order cycle TB 2.6 of Haq et al. (1988) starting at 12.7 Ma and ending at 11.6 Ma. The Badenian/Sarmatian boundary then would coincide with the glacio-eustatic isotope event MSI-3 (Abreu & Haddad 1998), and the Sarmatian/Pannonian boundary to the glacio-eustatic sea-level lowstand of cycle TB 3.1. Alternatively, Sen et al. (1999) proposed a date of 12.5 Ma for the beginning of cycle TB 2.6, suggesting an even younger age for the Badenian/Sarmatian boundary.

Data acquisition and processing

The well Spannberg-21 used for this study was drilled in 2007 by the Austrian oil and gas company OMV in the central part of the Vienna Basin (Fig. 1) with the objective of testing the so-called 15Z2 Tortonian horizon, a Middle Badenian basin floor fan (personal communication OMV). The well is located northeast on the Matzen-Spannberg ridge and reached a depth of approximately 2.0 km that covers the Middle to Upper Miocene. The first 450 m, covering the middle to Upper Pannonian, consist of mainly medium- to coarse-grained sandstones interbedded with siltstones and rare lignitic layers. The next 650 m cover the Lower Pannonian and the Upper Sarmatian and are more shale-rich with some thick, coarse-grained sandstone beds. Finally the last 900 m, covering the Lower Sarmatian and Badenian, consist of mainly heterolithic clastic sediments.

The drilling proceeded in two phases, with the first 450 m as a 12¼″ borehole, and the remaining 1529 m as an 8½″ borehole. The well was logged until 1837 m TVD with standard logging-while-drilling tools and additionally, for research purposes specifically designed for this study, with wireline logs that include high-resolution electrical borehole images (Formation Microscanner Imager, FMI, Mark of Schlumberger) as well as a paleomagnetic log with the Geological High-Resolution Magnetic Tool (GHMT, Mark of Schlumberger, now property of the Delft University of Technology).

The measurement principle of the GHMT is based on high-precision downhole measurements of the total magnetic field with a magnetometer, and of the susceptibility with an induction tool. When combining these two measurements with a measurement of the total Earth's magnetic field at a surface location close to the borehole, it is possible to derive the in-situ remanent magnetizations of the traversed sediments, in the form of scalar values that can then be correlated to the susceptibilities in order to obtain a sequence of polarity reversals (Luthi 2001). Correlating this sequence to the Geomagnetic Polarity Time Scale (GPTS) can result in magnetostratigraphic age dating (Pozzi et al. 1993; Thibal et al. 1999; Barthes et al. 1999; Williams 2006).

Conditions for the paleomagnetic logging tool were nearly ideal: the borehole diameters and temperatures were within tool specifications, and there was little pollution by magnetic particles in the mud. The paleomagnetic logging tool was run over both well intervals and two repeat runs were taken for quality control. The data was processed at the Schlumberger Riboud Product Centre (SRPC) using proprietary Schlumberger software. The whole well was used for the interpretation except for the uppermost 72 m and the interval between 454 and 480 m, where steel casing negatively influenced the magnetic measurements.

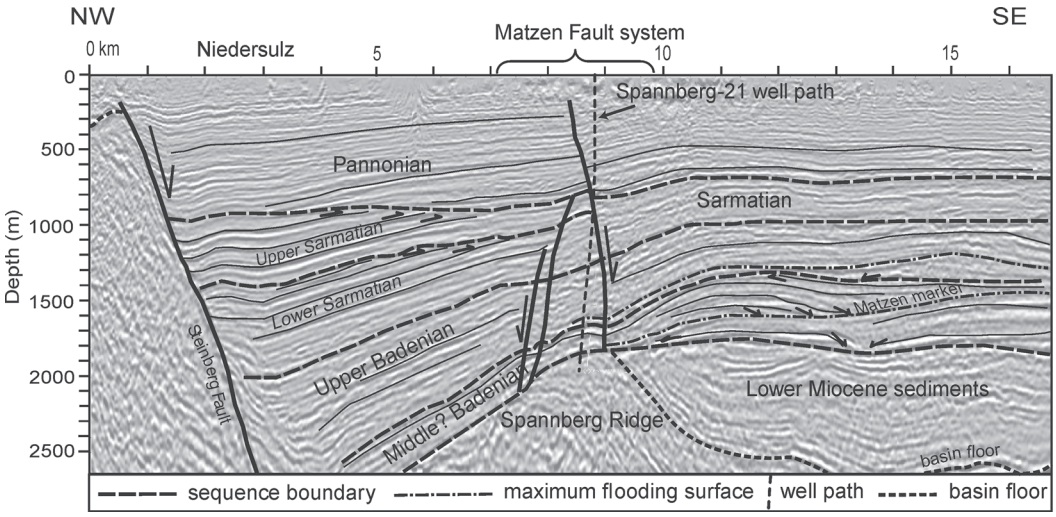

Fig. 3. A NW-SE oriented seismic section crossing the Spannberg-21 well and the Steinberg Fault (see stippled line in Fig. 1 for location) and the corresponding interpretation of the seismic section. Vertical exaggeration is approximately 1.6.

For the lithological characterization of the well, the operating company OMV sampled cuttings for the 8½″ section at a rate of one sample per 5 to 10 m. From the cutting material, 65 samples have been evaluated for their foraminiferal content in order to identify the regional biostratigraphic zones. The sample material was dried and soaked in diluted H_2O_2, wet sieved under running water and separated into two size-fractions: 63–125 µm and >125 µm. The larger fractions were analysed for all samples and the foraminifera were identified on the basis of the work by Papp & Schmid (1985), Cicha et al. (1998) and Schütz et al. (2007).

Calcareous nannoplankton from 55 cutting samples (740–1966 m TVD) was analysed on smear slides prepared using standard procedures and examined under a petrographic microscope. The lowermost part of the well (1927–1966 m) was found to be strongly contaminated with older, reworked microfossils.

The seismic lines were provided by OMV and originate from a 3-D pre-stack depth-migrated survey. They are aligned in a radial configuration around the well (Fig. 1).

Results

Seismic analysis

Figure 3 shows a seismic line crossing the well in a NW-SE direction, with the well location in the vicinity of the Matzen-Spannberg ridge, a SW-NE striking basement structure forming an anticlinal structure in the overlying Neogene section. The Matzen Fault System, which is in the proximity of the well, affects the quality of the seismics in this area and complicates the tracking of the reflectors across the faults.

Structural and stratigraphic framework

The NE-SW oriented Steinberg Fault (Fig. 3) is the largest fault in the Vienna Basin. According to Hinsch et al. (2005a) it reaches a maximum of 5.6 km throw and branches off the sinistral strike-slip faults at the basin border. Hinsch et al. (2005a) also showed that the Steinberg and Bockfliess Faults (the latter situated southwest of the Steinberg Fault, see Fig. 1) were the main active faults in the central Vienna Basin during the Early Sarmatian and the Early Pannonian. This is demonstrated by thick sediment accumulations northwest of the Matzen Fault System in the hanging wall of the south-east dipping Steinberg Fault (Fig. 3). The Matzen Fault System strikes SW-NE and consists of northwest- and southeast-dipping rotational faults with maximum throws of 80 m. In the vicinity of the Spannberg-21 well a network of smaller normal faults can be distinguished on the seismics (Fig. 3) but one significant normal fault can be identified that traverses the well close to the Pannonian-Sarmatian stage boundary, with an estimated throw of 70 meters.

The Badenian, Sarmatian and Pannonian sequence could be identified on the seismics (Fig. 3) using stratigraphic tie-ins from the biostratigraphical analysis. The seismic-to-well tie was established by creating a synthetic seismogram from the well logs that was subsequently correlated to the seismic traces at the well. An erosional unconformity is identified from seismics at the boundary between the Upper and Lower Sarmatian stage with an estimated missing thickness of approximately 160 m (Fig. 3). The Pannonian-Sarmatian boundary is recognized on the seismic section as a distinct unconformity, with the Sarmatian reflectors obliquely truncated to the NW of the well but disconformably overlying them to the SE (Fig. 3). The maximum eroded thickness, as estimated from seismics, is about 280 m.

Biostratigraphy

Foraminifera

The Badenian and Sarmatian biostratigraphy in the Central Paratethys is commonly based on assemblages of benthic foraminifera (Papp et al. 1978; Cicha et al. 1998). The Badenian is subdivided into a lower and upper Lagenid-Zone (Lower Badenian), a *Spiroplectammina*-Zone (Middle Badenian) and a *Bulimina-Bolivina*-Zone (Upper Badenian); the *Bulimina-Bolivina*-Zone is followed by sediments characterized by poorly diverse assemblages of *Ammonia*, *Quinqueloculina* and *Porosononion* (Papp et al. 1978; "*Ammonia*-zone" sensu Kováč et al. 2004 and Kováčová et al. 2008; Cicha et al. 1998). The Sarmatian is subdivided into the *Anomalinoides dividens*-, the *Elphidium reginum*-, the *Elphidium hauerinum*-Zones (all Lower Sarmatian) and the *Porosononion granosum*-Zone (Upper Sarmatian) (Cicha et al. 1998; Schütz et al. 2007) (Fig. 2). The lacustrine Pannonian sediments do not contain any foraminifera.

Although often poorly preserved, the benthic foraminifera from the cutting samples allow for a proper biostratigraphic evaluation. Samples from the lower part of the well (1999–1779 m) reveal impoverished assemblages with low numbers of specimens, mainly consisting of *Ammonia* spp. and *P. granosum*. The lack of any marker species does not allow a biostratigraphic assignment.

A distinct faunal change is documented in samples from 1790–1772 m. Species of *Bulimina* and *Bolivina* become dominant, accompanied by a diverse fauna including *Nonion commune*, *Valvulineria complanata*, *Gyroidinoides* sp., *Praeglobobulimina pyrula*, *Elphidium* sp., *Heterolepa dutemplei* and *Uvigerina* sp. The frequent occurrence of *Bolivina dilatata* cf. *maxima* suggests a Late Badenian age (Fig. 4), and the dominance of *Bolivina* spp. and *Bulimina* spp. as well as the absence of agglutinated species indicate the *Bulimina-Bolivina*-Zone. The overlying sediments (1772–1313 m) also correspond to the Upper Badenian. Foraminifera occur only in small numbers and consist of *Ammonia* sp., *Elphidium* sp., *Cibicidoides* sp., *Bulimina elongata elongata*, *Cycloforina* sp. as well as miliolids, indicating the "*Ammonia*-zone". The Badenian/Sarmatian boundary is difficult to detect as no distinctive change is observed in foraminiferal assemblages from 1304–1257 m. Foraminifera occur in small numbers with *Ammonia* sp. dominant, *Elphidium* spp. and miliolids common and *Anomalinoides* sp. rare in some samples.

An Early Sarmatian age is clearly indicated for samples from 1257–1104 m. They are dominated by *Ammonia* cf. *pseudobeccarii* and *Elphidium* spp. and — from 1257–1192 m — by

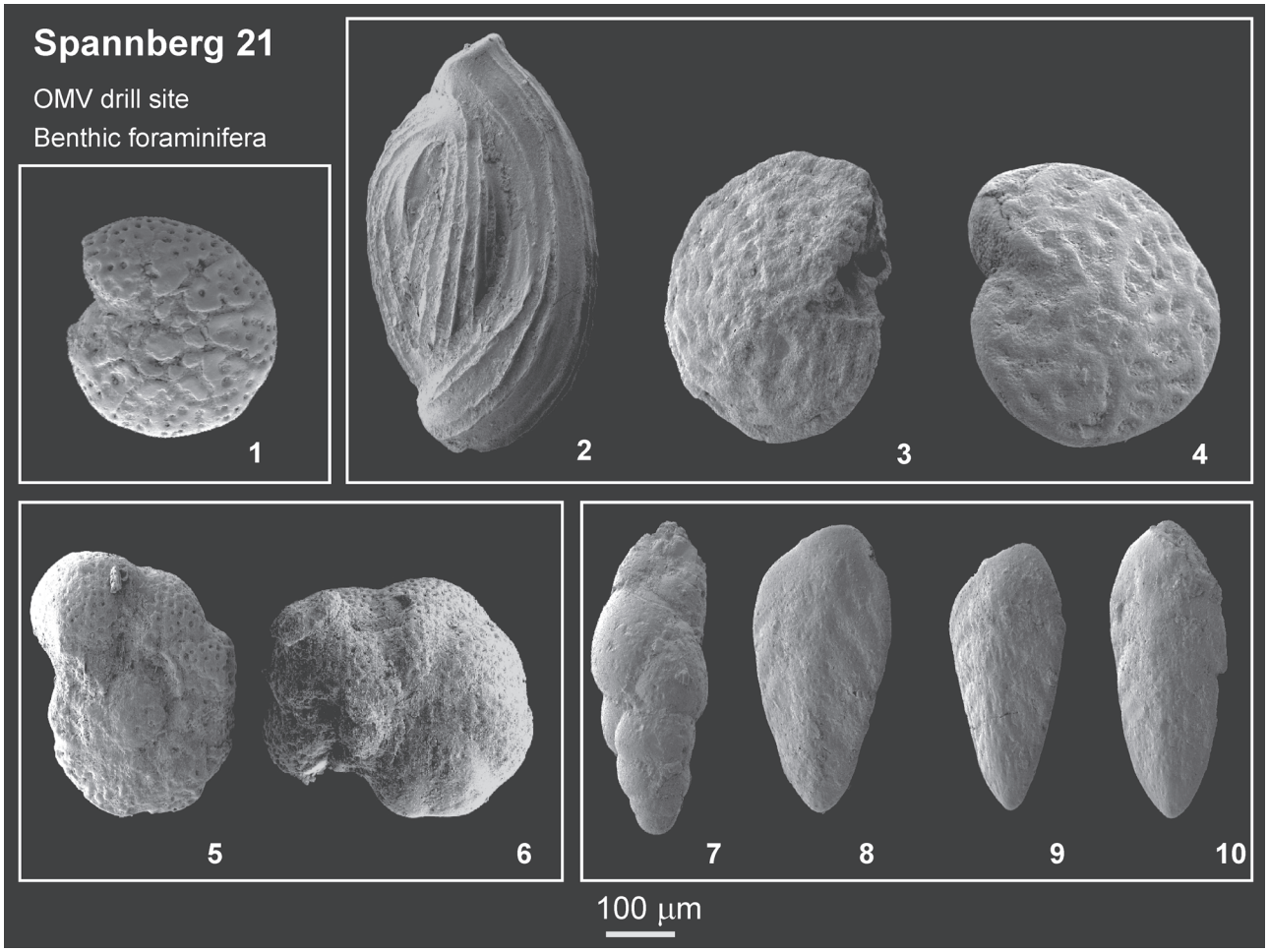

Fig. 4. Benthic foraminifera from the Spannberg-21 well. **1** — *Porosononion granosum*; sample 876–866 m. **2** — *Cycloforina karreri*; sample 1164–1155 m. **3–4** — *Elphidium* cf. *grilli*; sample 1164–1155 m. **5** — *Anomalinoides transcarpathicus*; sample 1202–1192 m. **6** — *Anomalinoides* cf. *dividens*; sample 1202–1192 m. **7** — *Bulimina elongata*; sample 1777–1772 m. **8–9** — *Bolivina dilatata* cf. *maxima*; sample 1777–1772 m. **10** — *Bolivina dilatata dilatata*; sample 1777–1772 m.

Anomalinoides spp. (Fig. 4); *P. granosum* occurs in low numbers in some of the samples. Miliolids like *Quinqueloculina* sp. and *Cycloforina karreri* occur regularly (Fig. 4), while *Hanzawaia boueana*, *Nonion* spp., and *Globigerina bulloides* occur in low numbers. A further subdivision of the Lower Sarmatian sequence is not possible due to the absence of characteristic elphiid biomarkers. Large elphiids like *E. reginum* are totally absent in all samples but some specimens of *E.* cf. *hauerinum* are present in samples from 1164–1104 m (Fig. 4).

The boundary between the Lower and Upper Sarmatian is indicated by a change in the faunal composition. Mass occurrences of *P. granosum* (often making up more than 90 % of the assemblage) suggest that the interval from 1104–866 m belongs to the *Porosononion granosum*-Zone (Fig. 4). Species of *Ammonia*, *Elphidium* and miliolids (*Quinqueloculina* sp., *Varidentalina reussi* — the latter only known from the Sarmatian; Schütz et al. 2007) occur in very low numbers in some of the samples (Fig. 4).

A Pannonian age of the upper part of the well (866–739 m) is indicated by the total absence of foraminifera. Samples often contain mollusc fragments, ostracods and coal/plant remains. The lowermost sample contains several specimens of *P. granosum* but they are heavily damaged and abraded and are thus most likely reworked during the initial Pannonian transgression (Kováč et al. 2004).

Calcareous nannoplankton

Numerous paleontologists (Kamptner 1948; Stradner & Fuchs 1978; Ćorić & Hohenegger 2008) have investigated the calcareous nannoplankton content of Middle Miocene sediments of the Austrian part of the Vienna Basin. The Badenian and Sarmatian regional stages span the nannoplankton zones upper NN4 to lower NN7 of Martini (1971) (Fig. 2). During the Pannonian the isolation of the Central Paratethys caused the development of an endemic nannoflora in Lake Pannon. Blooms of endemic nannoplankton are well known from the central part of Lake Pannon (Ćorić 2005), but in the Austrian part the Pannonian sediments mostly contain reworked taxa from older sediments. Pannonian endemic calcareous nannoplankton from the Austrian part of the Vienna

Basin is therefore only sporadically recorded (Peresson et al. 2005).

Sand-rich sediments from 1890–1723 m are characterized by a common and well preserved nannoflora with typical Early Miocene taxa: *Discoaster druggii* Bramlette & Wilcoxon, *Helicosphaera ampliaperta* Bramlette & Wilcoxon, *Helicosphaera mediterranea* Müller, *Reticulofenestra bisecta* (Hay) Roth, *Reticulofenestra excavata* Lehotayova, *Triquetrorhabdulus carinatus* Martini, whereas *Sphenolithus heteromorphus* Deflandre occurs only in sample 1774–1769 m. These nannoplankton assemblages belong to nannoplankton Zones NN1–NN4 (Lower Miocene) and were transported here from the North Alpine Foreland Basin during the Middle Badenian.

Strong contamination in the lower part of the investigated section (sample 1625–1616 m) is documented by the occurrences of the endemic Pannonian *Noelaerhabdus bozinovicae* Jerkovic. It is therefore not possible to make any further biostratigraphical subdivision of this part of the well. The common occurrence of species of the genus *Calcidiscus*, typical for NN6 (Fig. 2), was observed in sample 1239–1230 m. The larger morphotype (7 μm) of *Reticulofenestra pseudoumbilicus* (Gartner) Gartner was observed from 1294–895 m. An increase in the abundance of this form has been encountered in uppermost NN5 and NN6/NN7 in the Mediterranean area and was used for the biostratigraphic subdivision of the Miocene sediments in that region (Fornaciari et al. 1996). Nannoplankton assemblages in sample 866–856 m become rich and better preserved, containing Middle Miocene species but no zonal markers. The uppermost part of the well (866–740 m) contains very rare and biostratigraphically insignificant nannoplankton probably reworked from the older strata.

Magnetostratigraphy

The downhole paleomagnetic measurements proved to be of good quality with an excellent repeatability. The processed paleomagnetic logs showed clear polarity reversals for the post-Badenian intervals. In the Badenian interval the susceptibility signal and remanent magnetic signals are very low. However the remanent signal was well reproduced by the repeat measurement of the paleomagnetic logging tool, allowing for a determination of the polarities.

Figure 5 shows the polarity sequences obtained for the entire paleomagnetic well record. For the Badenian a reliable correlation to the GPTS is difficult and the correlation suggested in Fig. 5 is only possible if significant hiatus oc-

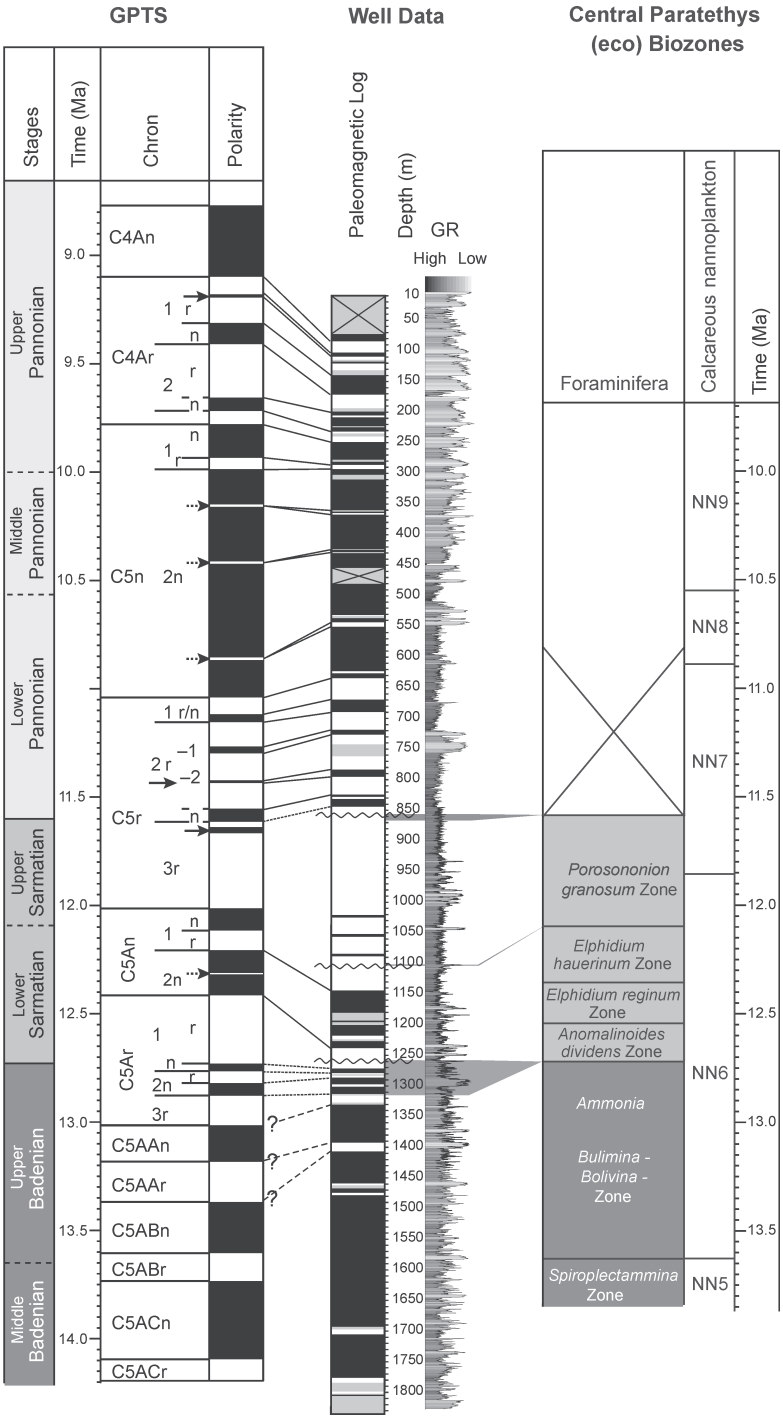

Fig. 5. Summary of the bio- and magnetostratigraphic results and their correlation to the GPTS (Lourens et al. 2004) and the Central Paratethyan biozones (foraminifera after Cicha et al. 1998 and calcareous nannoplankton after Lourens et al. 2004). Solid lines indicate correlations with high confidence; dotted lines indicate correlations with less certainty. Grey areas indicate the error bars for the biostratigraphic analysis. On the paleomagnetic log black represent normal polarity, white reversed polarity and grey uncertain polarity. The intervals with no paleomagnetic data are indicated with crosses. Solid arrows on the GPTS indicate the short polarity subchrons and dashed arrows indicate the location of the polarity fluctuations within Chron C5n.2n as described by Krijgsman & Kent (2004). The main unconformities in the well are indicated by an undulating line on the paleomagnetic log.

cur. Correlating the well polarity sequence to the GPTS for the Sarmatian is also not straightforward, but the long reverse period located in the biostratigraphically determined upper Sarmatian substage can be reliably linked to Subchron C5r.3r. The unconformity at the Lower to Upper Sarmatian stage boundary, determined from seismics, is interpreted as the explanation of the missing Chron C5An.1n. Therefore, the reverse polarity interval between 1144 m and 1104 m is interpreted as Subchron C5An.1r, and the normal interval below it as Subchron C5An.2n.

A good and detailed correlation to the GPTS can be made for the Pannonian (Fig. 5). Here even two short polarity subchrons could be identified that are not included in the most recent GPTS (Lourens et al. 2004) but have been described by Krijgsman & Kent (2004) as Subchron C4Ar.1r–1n and C5r.2r–2n. Three polarity fluctuations within Chron C5n.2n were also encountered in the paleomagnetic log at the expected locations (Krijgsman & Kent 2004) (dashed arrows in Fig. 5).

Regional well correlation of Sarmatian strata

Harzhauser & Piller (2004) conducted a correlation of the Sarmatian with wells located in the northern Vienna Basin and the Styrian Basin. Despite different sedimentation rates and different tectonic settings they identified similar well log patterns and were able to identify correlatable shale-rich intervals that they interpreted as basin-wide flooding surfaces. They found the most complete Sarmatian intervals in the wells Niedersulz-9 and Eichhorn-1 (Fig. 1) with a total estimated thickness of 1050 m in the first well, but an uncertain location of the Badenian-Sarmatian boundary due to microfaunal contamination. Earlier, Friedl (1936) and Papp (1974) had analysed the biozones in the Niedersulz-9 well, located ca. 9 km northeast of Spannberg-21, and Papp (1974) had proposed the well as a Sarmatian/Pannonian boundary stratotype. The Eichhorn-1 well is located approximately 15 km NNE of the Spannberg-21 well and Harzhauser & Piller (2004) found the

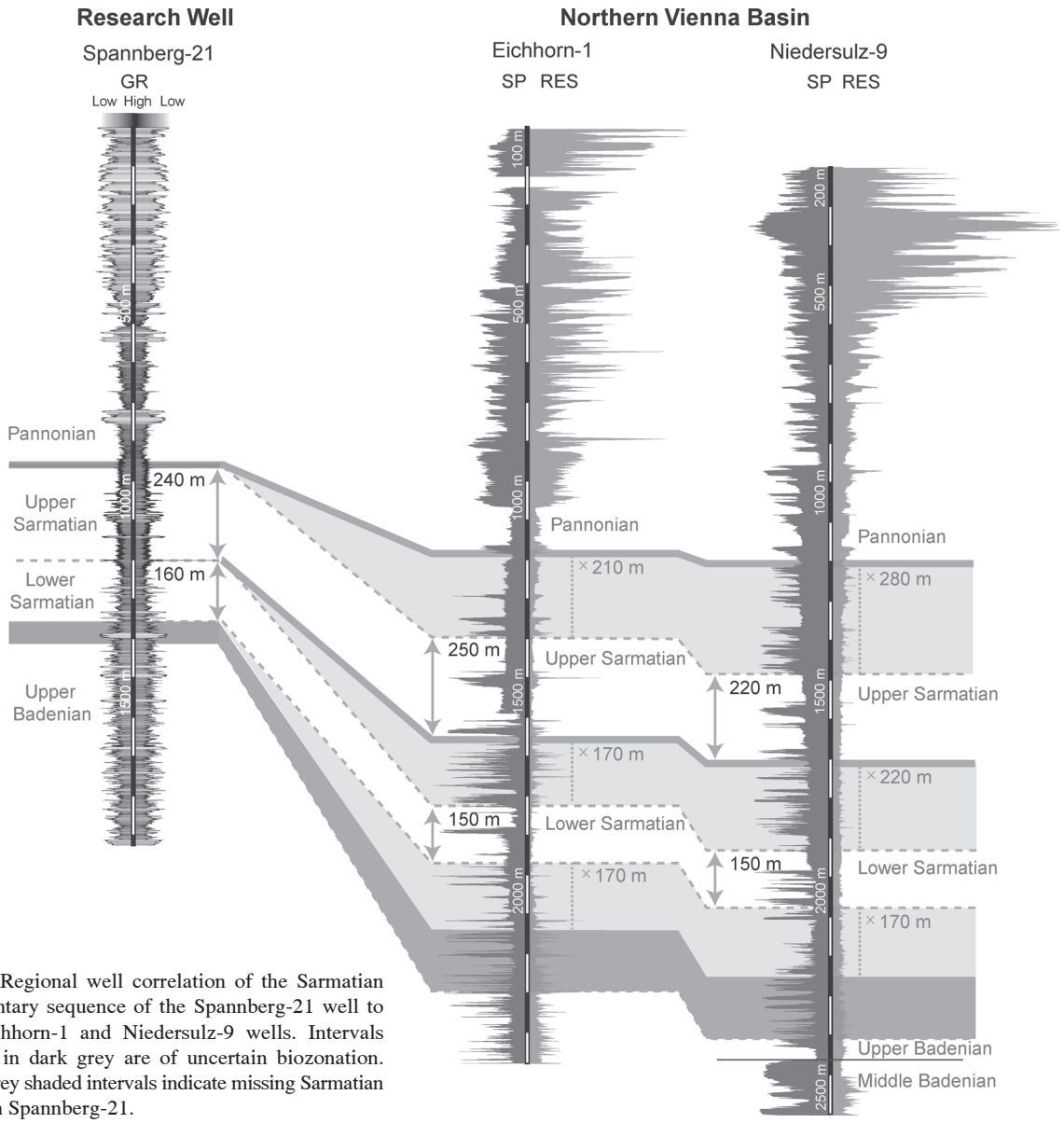

Fig. 6. Regional well correlation of the Sarmatian sedimentary sequence of the Spannberg-21 well to the Eichhorn-1 and Niedersulz-9 wells. Intervals shaded in dark grey are of uncertain biozonation. Light grey shaded intervals indicate missing Sarmatian strata in Spannberg-21.

Sarmatian to have a thickness of 1126 m ± 10 m. The biostratigraphy of the Eichhorn-1 well is based on molluscs and benthic foraminifera (Harzhauser et al. 2004).

The Sarmatian in Spannberg-21 is about 425 ± 35 m and therefore considerably thinner than the corresponding strata in the northern Vienna Basin. The reduced thicknesses of the Sarmatian in the Matzen area compared to the northern Vienna Basin is attributed by Harzhauser & Piller (2004) to the position on the intrabasinal Matzen-Spannberg ridge. To determine whether the Sarmatian in Spannberg-21 is a condensed section or whether there are missing intervals, a correlation was made to the Eichhorn-1 and Niedersulz-9 wells (Fig. 6). The correlation is based on shale marker beds that are distinguishable in the three wells. In the Lower Sarmatian of Spannberg-21 the shale interval at 1168–1115 m is used as a tie-in (Fig. 6). This interval is represented in the Vienna Basin and the Styrian Basin as a 50 m thick interval of grey marls, overlain by a succession with strongly serrated log responses, consisting of coarse sand, gravel and intercalations of thin pelitic layers with a total thickness of 195 m ± 25 m. This sequence cannot be identified in Spannberg-21, suggesting a stratigraphic gap and supporting the unconformity between the Upper and Lower Sarmatian substage boundaries interpreted from the seismics.

The section below the grey marl interval is about 160 m thick in Spannberg-21, considerably less than the 320 m reported from the wells in the northern Vienna Basin. This is likely to be the stratigraphic gap at the base of the Sarmatian that Harzhauser & Piller (2004) report for the Matzen area. It is difficult though to quantify how much of the Sarmatian strata is missing since the Badenian/Sarmatian boundary cannot be accurately determined in any of these wells.

In the Upper Sarmatian Harzhauser & Piller (2004) describe three basin-wide correlatable shale-rich intervals. In Spannberg-21, the lower two of these can be identified and correlated, but not the third one (Fig. 6). It is suggested that a missing section of 245 m ± 35 m occurs at the top of the Sarmatian, at a depth of 858.5 m where an erosional surface can be distinguished on the electrical borehole images. This is also supported by the discordant unconformity observed on the seismics, with an estimated missing section of 280 m.

Sedimentation rates

Using the chronostratigraphic tie-ins and the stratigraphic gaps identified in Spannberg-21, a detailed plot of age versus depth is constructed for the Pannonian and Sarmatian (Fig. 7). Data points include biostratigraphic and magnetostratigraphic tie-ins as well as the presumed missing sections. The dashed lines in Figure 7 are interpolated or fitted between the various data points and indicate the sedimentation rates per interval. The numbers next to these intervals are the resulting sedimentation rates in metes per thousand years (kyr), with corrections for tectonic dip but not for compaction. The sedimentation rates for the Badenian are difficult to determine for lack of reliable chronostratigraphic markers.

The sedimentation rate is 0.43 m/kyr in the Lower Sarmatian and then shows a remarkable increase in the Upper Sarmatian to more than 1.2 m/kyr. In the Pannonian the sedimentation rate decreases to fairly constant values, initially to 0.36 m/kyr and in the upper half to 0.30 m/kyr. At a depth of 190–180 meters a shift in the line connecting the paleomagnetic tie-in points suggests another stratigraphic gap in the sedimentary record with an estimated duration of 200 kyr that had not been identified by the other methods (Fig. 7).

Discussion and conclusions

The high-resolution borehole record of the Miocene in the central part of the Vienna Basin reported in this study is obtained through a combination of stratigraphic methods. It allows an accurate determination of sedimentation rates, depending on the number of tie-in points, as well as the identification of stratigraphic gaps and their duration. The good agreement between the biostratigraphical and the paleomagnetic data of the post-Badenian sequence, augmented by information gained from seismic and borehole images, is a strong argument for the validity of the record. A discussion of the results for each regional stage is provided in the following section.

Badenian

In the neighbourhood of the Spannberg-21 well and east of the Austrian-Slovak border, Kováč et al. (2004) described three 3rd order cycles in the Badenian, approximately corresponding to the Lower, "middle" and Upper Badenian. They suggested that the Upper Badenian cycle could have been controlled by sea-level changes outside the Central Paratethys realm and therefore correlated this cycle with the global sea-level cycle TB 2.5 (12.75–13.65 Myr). In the Matzen Field the Middle/Upper Badenian sequence boundary was also recognized by Fuchs & Hamilton (2006), who attributed a sea-level drop to the 9th Tortonian horizon where the shelf edge advanced about 2 km southward.

In the Spannberg-21 well, a detailed stratigraphic analysis in the Badenian is hampered by the paucity and probable reworking of microfossils, and the difficulty of interpreting the palaeomagnetic record. The latter is obtained from a weak yet repeatable signal from the paleomagnetic log, but the predominantly normal polarities extracted from it are difficult to reconcile with the GPTS, particularly because of the apparent absence of Chrons C5AAr and C5ABr (Fig. 5). The foraminiferal assemblages suggest a Late Badenian age down to a depth of at least 1790 m. Sequence stratigraphic considerations provide assistance in the stratigraphic control of the Badenian in the Matzen area. The upper two Badenian 3rd order cycles can be recognized on the seismic line in Figure 3. The "middle" Badenian cycle comprises the Middle Badenian transgressive systems tract (TST) which can be recognized by onlapping reflectors (the Matzen sands or 16th Tortonian horizon of Kreutzer (1986)) onto the basin floor. Furthermore the maximum flooding surface (MFS), also referred to as the Matzen Hauptmarker (Kreutzer 1986; Fuchs & Hamilton 2006), can be distinguished by the downlapping reflectors of the following prograding highstand sequence tract (HST). In Spannberg-21 this Matzen Hauptmarker immediately under-

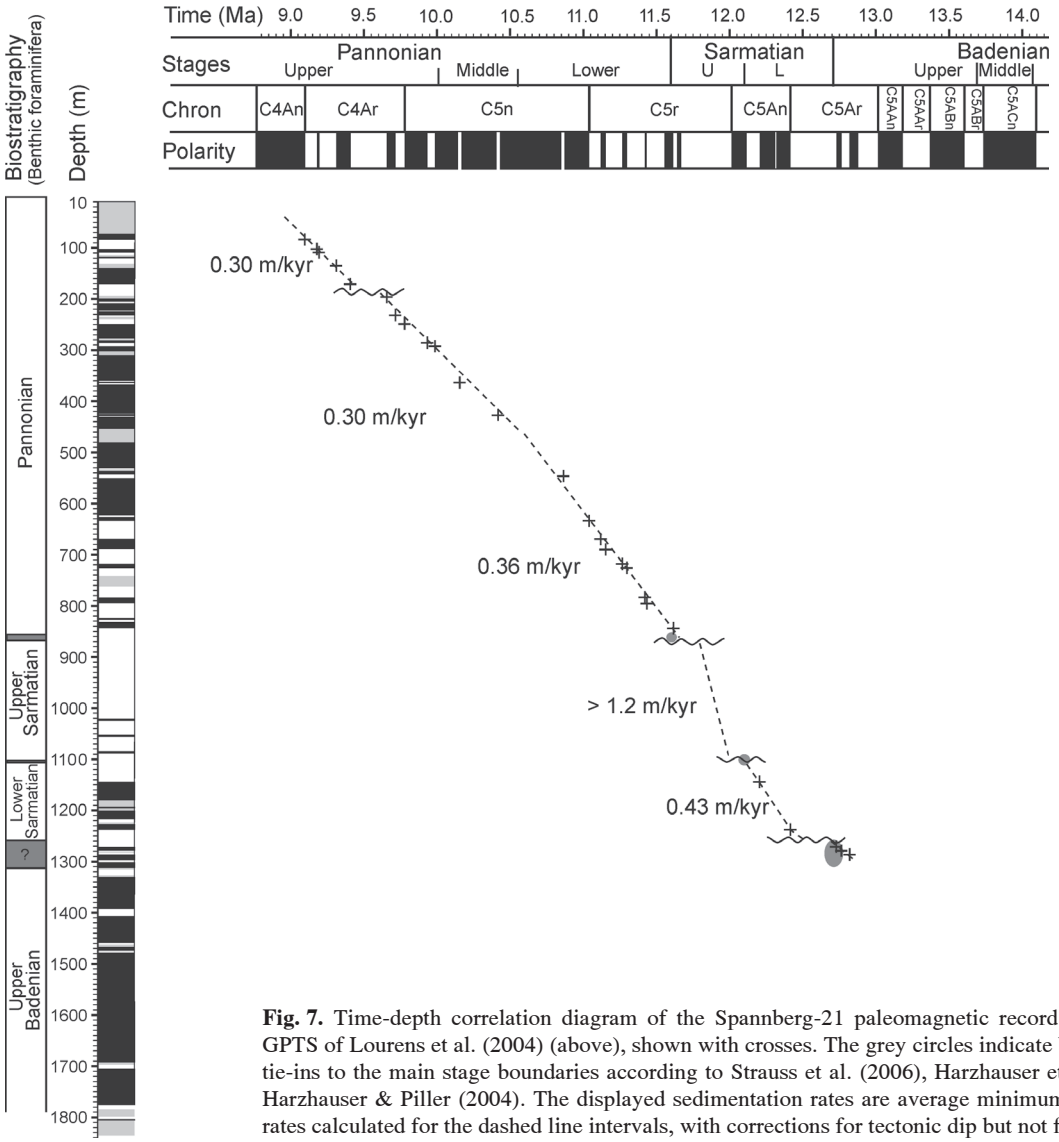

Fig. 7. Time-depth correlation diagram of the Spannberg-21 paleomagnetic record (left) with the GPTS of Lourens et al. (2004) (above), shown with crosses. The grey circles indicate biostratigraphic tie-ins to the main stage boundaries according to Strauss et al. (2006), Harzhauser et al. (2004) and Harzhauser & Piller (2004). The displayed sedimentation rates are average minimum sedimentation rates calculated for the dashed line intervals, with corrections for tectonic dip but not for compaction.

lies the targeted fan (pers. comm. OMV) and the targeted sands are therefore considered to be part of the Middle Badenian HST. In Figure 3 this HST can be seen to the Southeast of the well as a system with prograding clinoforms in line with Hamilton & Johnson (1999), interpreted as delta plain, delta front and slope deposits. The seismics additionally shows some toplap truncations terminating at the sequence boundary that, in line with Kováč et al. (2004), is interpreted as the boundary between the Middle and the Upper Badenian. In the Spannberg-21 well this horizon is identified at 1612 m (9th Tortonian horizon, pers. comm. OMV). This seismic stratigraphic boundary is located considerably higher than the foraminiferal *Bulimina-Bolivina* Zone that placed the Upper Badenian boundary at 1790 m or deeper. This contradiction between well log stratigraphy, seismic stratigraphy and the use of foraminiferal zones to determine the Upper/Middle Badenian boundary has already been noted by Kováč et al. (2004). After the base level drop, during the following Upper Badenian LST, the depocentres shift basinward, forming clinoforms with a progradational to aggradational stacking pattern. This sequence seems to be present only in a highly condensed form in Spannberg-21. In conclusion the Spannberg-21 well is interpreted as comprising the Upper Badenian 3rd order sequence and the HST of the "middle" Badenian cycle, in agreement with the sequence stratigraphic framework proposed by Strauss et al. (2006) and Kováč et al. (2004). The partly condensed nature of the sequence, which is attributed to the position on an intrabasinal high, and the possible stratigraphic gaps are thought to account for the difficulty of linking the paleomagnetic well record to the GPTS.

Sarmatian

Previous authors (Harzhauser & Piller 2004; Strauss et al. 2006; Kováč et al. 2008) have proposed a sequence stratigraphic framework for the Sarmatian in the Vienna Basin with a 3rd order cycle spanning the entire Sarmatian and two 4th order cycles corresponding as the Lower and Upper Sarmatian respectively. The sedimentation during the first 4th order cycle is reported to be mainly siliciclastic and, according to

Harzhauser et al. (2004), its TST is modulated by several transgessive pulses. Kreutzer (1974) interprets the MFS as coinciding with that of the 3rd order cycle and during the following HST significant fan deltas were deposited in the central Vienna Basin. Harzhauser et al. (2004) mark the sequence boundary above it as the transition from the Lower to the Upper Sarmatian, characterized in marginal and topographically exposed settings by extensive erosion that removed most of the *Elphidium hauerinum* Zone. They characterized the deposition during the second 4th order cycle as mixed siliciclastic-oolitic and comprising the Upper Sarmatian substage. During its TST previously exposed marginal areas of the basin were flooded. Furthermore Harzhauser et al. (2004) found that the subsequent MFS can be identified on all well logs in the Vienna Basin. The upper 4th order HST comprises also the upper part of the *Porosononion granosum* Zone, but complete records are only reported from boreholes, because along the margins and in exposed areas the uppermost Sarmatian has been completely eroded. Finally Kováč et al. (1998a) recognized deep valley incisions and erosion at the Sarmatian/Pannonian (Serravallian/Tortonian) boundary and interpreted this as a type 1 sequence boundary.

The results in Spannberg-21 allow us to place the Sarmatian sequence in an accurate stratigraphic framework. Sedimentation rates increase significantly between the Lower and Upper Sarmatian from 0.43 m/kyr to more than 1.2 m/kyr. Stratigraphic gaps are found at the base of the Sarmatian, at the boundary between the Lower and Upper Sarmatian, as well as at the top. Magnetostratigraphic control places the Badenian/Sarmatian boundary at about 1260 m in the well, but the strongly reduced presence of Chron C5Ar.1r and the well correlation suggest a time gap of about 250 kyr. The other two stratigraphic gaps, between the Upper and Lower Sarmatian and at the top of the Sarmatian, have an estimated time gap of 69–95 kyr and 180–210 kyr respectively amounting to a total missing time in the Sarmatian between 490 and 570 kyr. These results provide a basis for a link with the existing sequence stratigraphic framework of the Sarmatian. The Lower Sarmatian strata in Spannberg-21 start slightly above 12.5 Ma with the TST, and the following MFS of the 3rd order cycle expressed by the shaly interval at 1168–1115 m is situated in Chron C5An.1r (12.2–12.15 Ma). The subsequent HST is not clearly represented in the well, most probably because of the stratigraphic gap between the Upper and Lower Sarmatian. The Upper Sarmatian starts with the 4th order TST at 1100 m and the subsequent MFS at 920 m, approximately between 12.0 and 11.8 Ma. The final 4th order HST is part of the stratigraphic gap identified at the Sarmatian/Pannonian boundary. The occurrence of the three stratigraphic gaps is attributed to the relative position on an intrabasinal high that made this area sensitive to eustatic sea-level changes, resulting in erosion during relative sea-level lowstands.

Pannonian

Papp (1951) subdivided the Pannonian of the Vienna Basin into eight biostratigraphic zones, termed A to H, based on the evolutionary levels of endemic molluscs. Kováč et al. (1998a) interpreted zones A–C as deltaic, zones D–E as offshore-dominated, and zones F–H as limnic with occasional floodplain deposits and coals. The onset of zone F was the time when according to Harzhauser et al. (2004) and Kováč et al. (2004) the Vienna Basin became permanently separated from Lake Pannon and a sedimentary gap was described between zones F and G.

Correlation of the Spannberg-21 logs with the Eichhorn-1 zonation by Harzhauser et al. (2004) resulted in the Papp zones indicated on Figure 8. Since the mollusc fragments in the cuttings of Spannberg-21 were too damaged by the drilling process to verify the biozone-correlation, this zonation is purely lithostratigraphic. The paleomagnetic results allow for a very accurate age dating of the Pannonian sequence in Spannberg-21, partly because of a strong remanent magnetization signal, but also because of the abundance of polarity reversals in the Pannonian and the continuous sedimentary record in the well. The paleomagnetic measurements were of sufficiently high resolution to allow identification of some short chrons or excursions that have been described by Krijgsman & Kent (2004) but are not yet included in the GPTS (Lourens et al. 2004). The Pannonian/Sarmatian (Serravallian/Tortonian) boundary is located in the lower part of — or slightly below — Chron C5r.2n (11.614–11.554 Ma). Complications caused by a fault crossing the well in Spannberg-21 and the erosive unconformity at the boundary make it difficult to assign an accurate depth and age for the onset of the Pannonian in this part of the basin, but a best estimate puts it at 858.5 m with an age of 11.6 Ma. The high number of tie-ins with the GPTS (Fig. 5) allow for an accurate estimation of the sedimentation rates in the Pannonian (Fig. 7). During the Early Pannonian this is found to be on average 0.36 m/kyr and decreases to about 0.30 m/kyr from 10.6 Ma onwards (at a well depth of about 480 m). This decrease in sedimentation rate in Spannberg-21 occurred at a time when distal deltaic deposition was followed by more proximal deposition related to the transition from Papp's (1951) zone C to zone D. At a depth of about 300 m, equivalent to an age of 10–9.9 Ma, the log signatures of the sand layers change from predominantly coarsening-upward, typical for mouth bars in delta-front deposits, to fining-upward with sharp bases, typical for channel deposits in deltaic and fluvial systems. Plant-rootlets identified on the electrical borehole images suggest a terrestrial environment, interpreted as the onset of zone F (Papp 1951) and also referred to as the lignitic series. Between 9.6–9.4 Ma the Spannberg-21 data indicate a stratigraphic gap (Fig. 7), above which there is a sequence of fining-upward, cross-bedded sandstone beds up to 15–20 m thick and often with erosional bases, interpreted as fluvial channels. The stratigraphic break is correlated to the transition from Papp's (1951) zone F to zone G.

Implications for basin evolution

The findings of this study can be placed in the context of the tectonic history of the Vienna Basin and its surroundings, and the global eustasy record. The sequence considered here is post-Karpatian and therefore focuses on the pull-apart phase of the basin. The seismic line in Figure 3 suggests that in the Middle Badenian major accumulations were deposited to the SE of the Spannberg ridge and prograded towards the SE,

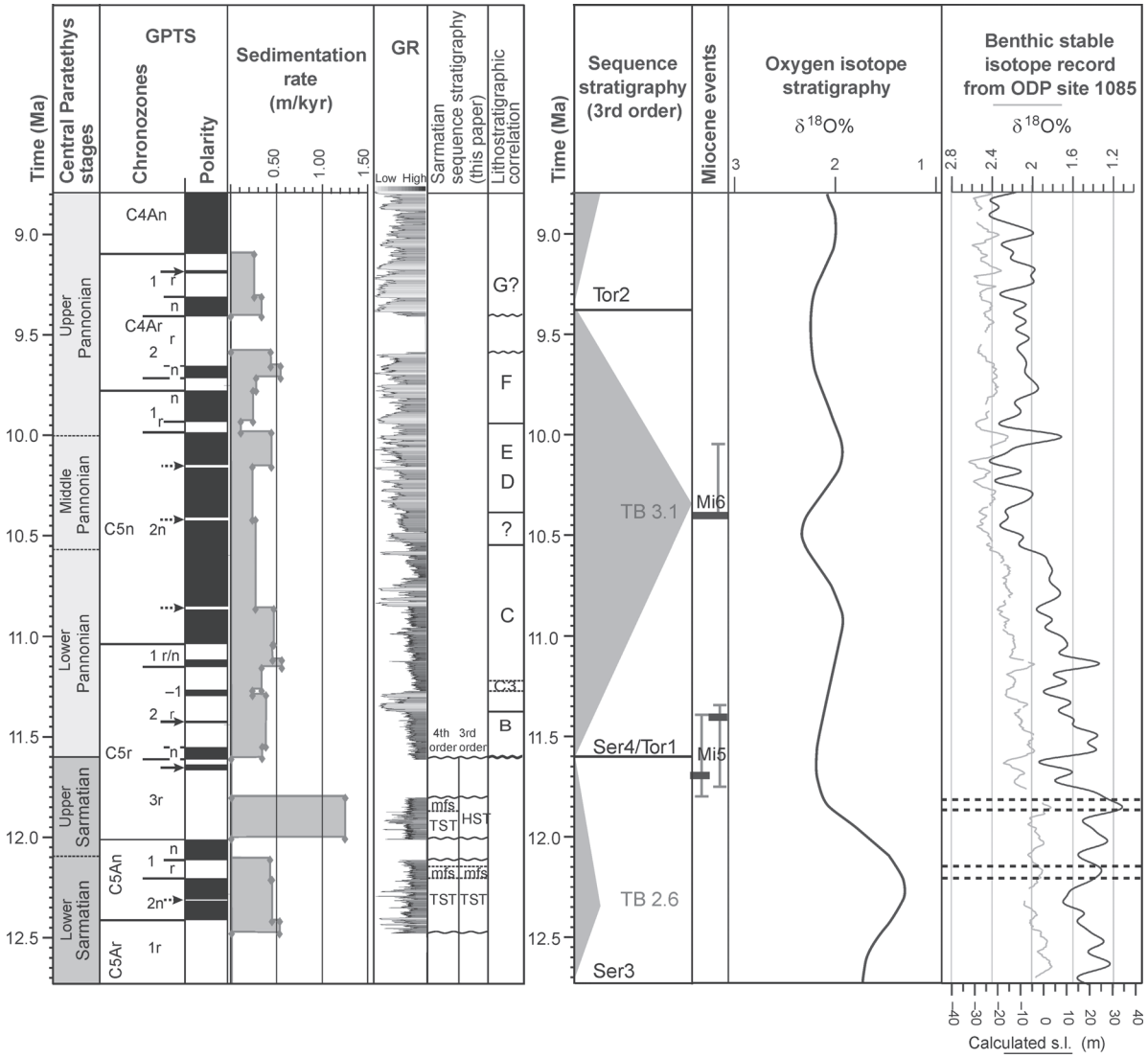

Fig. 8. Stratigraphy of the Spannberg-21 well based on seismic data, well correlation, biostratigraphy and magnetostratigraphy for the Sarmatian and Pannonian interval compared to standard stratigraphy and plotted versus time. The Central Paratethyan stages are according Strauss et al. (2006), Harzhauser et al. (2004) and Harzhauser & Piller (2004) and the GPTS according to Lourens et al. (2004). The sedimentation rates are calculated for the magnetostratigraphic intervals and are corrected for tectonic dip but not for compaction. The gamma-ray log was stretched linearly between the magnetostratigraphic tie-ins with the stratigraphic gaps taken into account. Lithostratigraphic correlation of the Pannonian is based on Harzhauser et al. (2004) using the biozone-correlation of Papp (1951). The 3rd order cycles are after Hardenbol et al. (1998), the Miocene isotopic events Mi5 and Mi6 according to Turco et al. (2001) and Westerhold et al. (2005) and the oxygen isotope stratigraphy from Abreu & Haddad (1998). Global glacioeustatic sea-level changes are derived from the $\delta^{18}O$ record of ODP Site 1085 (Westerhold et al. 2005) with dashed horizontal lines indicating the corresponding timing of the 4th order MFS in the Sarmatian interval in Spannberg-21.

while from the Late Badenian onwards significant accommodation space was created between the Spannberg ridge and the Steinberg Fault, mostly because of an increased activity of the latter due to pull-apart tectonics. Thicknesses of the Upper Badenian and Sarmatian in this area are 2–3 times higher than on the Spannberg ridge. The increased sedimentation rates during the Sarmatian (particularly in the Upper Sarmatian) found in this study suggest that the basin subsidence and the creation of accomodation space also extended to the relative high of the Spannberg ridge, although not to the same degree as in the adjacent areas. The Spannberg ridge, in fact, seems to have acted as a hinge area, with a tilt to the SE in the Middle Badenian followed by a downward pivoting of the area to the NW of the ridge, forming a half-graben between the Steinberg Fault and the Spannberg ridge. In the Pannonian, by contrast, the sedimentary thicknesses are more constant throughout the area, indicating a reduced activity of the Steinberg Fault and a more aggradational infill of the basin in its last phase. The basin infill in this area therefore closely reflects the tectonic development of the Vienna Basin, and this is also reflected in an overall coarsening-upward sequence as shown by the gamma ray log of the Spannberg-21 well in Fig. 5.

In order to analyse whether eustasy also played a role in the basin infill the calculated sedimentation rates in Spannberg-21

were used to construct a log as a function of time (Fig. 8). The gamma ray log is stretched linearly between tie-in points (Fig. 7), and stratigraphic time gaps are blanked out. This depth-time converted log is compared in Figure 8 to the 3rd order cycles of Hardenbol et al. (1998), the oxygen isotope curves from Abreu & Haddad (1998) and the short periods of glaciation in the Miocene (so called Mi-events) described by Miller et al. (1991), which were further refined by Turco et al. (2001) and Westerhold et al. (2005). The latter also converted the $\delta^{18}O$ record retrieved from ODP site 1085 into a record of sea-level changes by applying a gradient of 0.11 ‰ for a 10 m change in sea level, using the linear equation of Bemis et al. (1998) and assuming a 3 °C cooling of deep waters (Fig. 8).

There is no obvious relationship between lithology and sedimentation rates in Figure 8. The two MFS of the two Sarmatian 4th order cycles (indicated by mfs in Fig. 8) are seen to correspond to two minima in the $\delta^{18}O$ record and thus to the global glacio-eustatic highstands of Westerhold et al. (2005). The MFS of the Lower Sarmatian cycle also corresponds to a $\delta^{18}O$ minimum of Abreu & Haddad (1998). The following sea-level lowstand expressed in the ODP 1085 record across the Ser4/Tor1 boundary as well as in the isotopic record of Abreu & Haddad (1998) is found to coincide with the 3rd order lowstand in the Upper Sarmatian. An alternative explanation of the Sarmatian 4th order cycles proposed by Harzhauser & Piller (2004), is that they were caused by tectonic modulations due to an increased uplift of the Alps. The latter is roughly coeval with the Paratethyan retreat from the North Alpine Foreland Basin, which resulted in increasing amounts of coarser sediment from the Alps being shed into the Vienna Basin. This accelerated tectonic activity is reflected in our data by the high sedimentation rates during the Late Sarmatian and the movement of the Steinberg Fault.

The onset of the Pannonian coincides with the Ser4/Tor1 boundary, namely the glacio-eustatic sea-level lowstand at the onset of the TB 3.1 cycle. At the end of this cycle, the Tor2 boundary coincides with the change of the sedimentary environment from deltaic to terrestrial at 9.6–9.4 Ma, coeval with the transition from zone F to zone G. Papp's (1951) zones A to F can thus be considered to comprise an entire 3rd order cycle in accordance with Harzhauser et al. (2004). The question remains whether this 3rd order cycle should be directly related to the TB 3.1 cycle because Lake Pannon, and therefore also the Vienna Basin, had probably lost its connection to the global seas for that time (Kázmér 1990; Rögl 1999; Magyar et al. 1999). Juhász et al. (2007) discussed different models for the response of fluvio-deltaic systems in the Pannonian Basin to tectonic and climatic controls and concluded that the 3rd order cycles are mainly driven by regional scale tectonic changes and that only the 4th- and higher order cycles may be driven by climatic cycles of the Milankovitch band. A climatic control for the 3rd order stratigraphic boundary could be argued based on the work of Böhme et al. (2008) who established a long proxy record of precipitation for Southwest and Central Europe for the Middle to Late Miocene. They described a "washhouse climate" (10.2–9.8 Ma) characterized by warm global conditions and high levels of precipitation followed by a period of relatively low precipitation (9.7–9.2 Ma) that corresponded to a cool global event (Westerhold et al. 2005; Winkler et al. 2002). These two phases match well with the evolution of Lake Pannon since during the "washhouse climate" the lake reached its maximum extent at approximately 10.5–10 Ma (Harzhauser et al. 2008) and the stratigraphic gap of 9.6–9.4 Ma encountered in Spannberg-21 coincides with the subsequent Central European dry period. The same climatic argument can be used for the transition from the distal to proximal deltaic setting, dated at 10.4–10.6 Ma where the average sedimentation rates decrease from 0.36 to 0.30 m/kyr. This could be linked to a punctuated period of global climate cooling, the Mi6 event that was astronomically dated at 10.4 Ma by Turco et al. (2001) and Westerhold et al. (2005) (Fig. 8). The detailed sedimentation rates shown on Figure 8 decrease from 0.47 m/kyr in the preceding Lower Pannonian to 0.27 m/kyr during this period of global sea-level lowstand. This interpretation could be validated if such an event was found to be coeval across the basin, but if found to be heterochronous it might have to be attributed to a progradational basin infill.

In conclusion, the data presented herein suggest that the infill history of the Vienna Basin is controlled by regional tectonic activity, but modulated by eustatic influences. The latter are most pronounced during times of greatest subsidence of the basin and full connectivity with the Paratethyan Sea and Lake Pannon respectively. In the later stages of the basin infill, when subsidence slowed and the connectivity to the Pannonian basins complex was no longer fully and permanently established, the eustatic signal is more difficult to detect and may have been driven by the coupling of global climatic processes that caused global eustatic sea-level variations. Thereafter, much of the Vienna Basin was essentially filled, subsidence ceased and much sediment was by-passed towards the Pannonian Basin to the Southeast and further down the basin drainage.

Acknowledgments: This research is supported by the Netherlands Research Centre for Integrated Solid Earth Science (ISES). We would like to thank Miroslav Pereszlényi and András Uhrin as well as two anonymous referees, whose comments significantly improved the manuscript. We are grateful to OMV for access to the well and for permission to publish the results, and in particular to Jost Püttmann for facilitating this study. OMV and Schlumberger Wireline Services are thanked for financial support. Furthermore we thank LETI/CEA and Geo-Energy for allowing the acquisition of the GHMT-tool and help in the transfer of knowledge. Finally Schlumberger is thanked for the in-house software to process the GHMT data and for providing the Geoframe and Petrel software.

References

Abreu V.S. & Haddad G.A. 1998: Glacioeustatic fluctuations: The mechanism linking stable isotope events and sequence stratigraphy from the Early Oligocene to Middle Miocene. *SEPM Spec. Publ.* 60, 245–259.

Barthes V., Pozzi J.P., Vibert-Charbonnel P., Thibal J. & Melieres M.A. 1999: High-resolution chronostratigraphy from downhole susceptibility logging tuned by palaeoclimatic orbital frequencies. *Earth Planet. Sci. Lett.* 165, 1, 97–116.

Bemis B.E., Spero H.J., Bijma J. & Lea D.W. 1998: Reevaluation of the oxygen isotopic composition of planktonic foraminifera: Experimental results and revised paleotemperature equations. *Paleoceanography* 13, 2, 150–160.

Böhme M., Ilg A. & Winklhofer M. 2008: Late Miocene "washhouse" climate in Europe. *Earth Planet. Sci. Lett.* 275, 3–4, 393–401.

Cicha I. 1998: The Vienna Basin. In: Cicha I., Rögl F., Rupp C. & Čtyroká J. (Eds.): Oligocene–Miocene foraminifera of the Central Paratethys. *Abh. Senckenberg. Naturforsch. Gesell.* 549, 43–45.

Cicha I., Rögl F., Rupp C. & Čtyroká J. 1998: Oligocene–Miocene foraminifera of the Central Paratethys. *Abh. Senckenberg. Naturforsch. Gesell.*, 549.

Cloetingh S. & Lankreijer A. 2001: Lithospheric memory and stress field controls on polyphase deformation of the Pannonian basin-Carpathian system. *Mar. Petrol. Geol.* 18, 1, 3–11.

Ćorić S. 2005: Endemic Sarmatian and Pannonian calcareous nannoplankton from the Central Paratethys. *12th Congress RCMNS*, 6–11, September 2005, Vienna, Abstract Volume, 53–54.

Ćorić S. & Hohenegger J. 2008: Quantitative analyses of calcareous nannoplankton assemblages from the Baden-Sooss section (Middle Miocene of Vienna Basin, Austria). *Geol. Carpathica* 59, 5, 447–460.

Decker K. & Peresson H. 1996: Tertiary kinematics in the Alpine-Carpathian-Pannonian system: links between thrusting, transform faulting and crustal extension. In: Wessely G. & Liebl W. (Eds.): Oil and gas in Alpidic Thrustbelts and basins of Central and Eastern Europe. *EAGE Spec. Publ.* 5, 69–77.

Decker K., Peresson H. & Hinsch R. 2005: Active tectonics and Quaternary basin formation along the Vienna Basin Transform fault. *Quat. Sci. Rev.* 24, 3–4, 305–320.

Fodor L. 1995: From transpression to transtension — Oligocene Miocene structural evolution of the Vienna Basin and the East Alpine Western Carpathian junction. *Tectonophysics* 242, 1–2, 151–182.

Fornaciari E., Di Stefano A., Rio D. & Negri A. 1996: Middle Miocene calcareous nannofossil biostratigraphy in the Mediterranean region. *Micropaleontology* 42, 1, 37–63.

Friedl K. 1936: Der Steinberg-Dom bei Zistersdorf und sein Ölfeld. *Mitt. Geol. Gesell., Wien* 29, 21–290.

Fuchs R. & Hamilton W. 2006: New depositional architecture for an old giant: the Matzen Field, Austria. In: Golonka J. & Picha F.J. (Eds.): The Carpathians and their foreland: Geology and hydrocarbon resources. *AAPG Mem.* 84, 205–219.

Hamilton W. & Johnson N. 1999: The Matzen project — rejuvenation of a mature field. *Petrol. Geosci.* 5, 2, 119–125.

Haq B.U., Hardenbol J. & Vail P.R. 1988: Mesozoic and Cenozoic chronostratigraphy and cycles of sea level changes. In: Wilgus C.K., Hastings B.S., Kendall C.G.S., Posamentier H.W., Ross C.A. & Van Wagoner J.C. (Eds.): Sea-level changes — an integrated approach. *SEPM Spec. Publ.*, 71–108.

Hardenbol J., Thierry J., Farley M.B., Jacquin T., Graciansky P.-C. & Vail P.R. 1998: Mesozoic and Cenozoic sequence chronostratigraphic framework of European basins. In: Graciansky C.-P., Hardenbol J., Jacquin T. & Vail P.R. (Eds.): Mesozoic and Cenozoic sequence stratigraphy of European basins. *SEPM Spec. Publ.* 60, 3–13.

Harzhauser M. & Kowalke T. 2004: Survey of the Nassariid Gastropods in the Neogene Paratethys. *Arch. Molluskenkunde* 133, 1–63.

Harzhauser M. & Mandic O. 2008: Neogene lake systems of Central and South-Eastern Europe: Faunal diversity, gradients and interrelations. *Palaeogeogr. Palaeoclimatol. Palaeoecol.* 260, 417–434.

Harzhauser M. & Piller W.E. 2004: Integrated stratigraphy of the Sarmatian (Upper Middle Miocene) in the western Central Paratethys. *Stratigraphy* 1, 1, 65–86.

Harzhauser M., Daxner-Höck G. & Piller W.E. 2004: An integrated stratigraphy of the Pannonian (Late Miocene) in the Vienna Basin. *Austrian J. Earth Sci.* 95/96, 6–19.

Harzhauser M., Kern A., Soliman A., Minati K., Piller W.E., Danielopol D.L. & Zuschin M. 2008: Centennial- to decadal scale environmental shifts in and around Lake Pannon (Vienna Basin) related to a major Late Miocene lake level rise. *Palaeogeogr. Palaeoclimatol. Palaeoecol.* 270, 1–2, 102–115.

Hinsch R., Decker K. & Peresson H. 2005a: 3-D seismic interpretation and structural modeling in the Vienna Basin: implications for Miocene to recent kinematics. *Austrian J. Earth Sci.* 97, 38–50.

Hinsch R., Decker K. & Wagreich M. 2005b: 3-D mapping of segmented active faults in the southern Vienna Basin. *Quat. Sci. Rev.* 24, 3–4, 321–336.

Hölzel M., Decker K., Zamolyi A., Strauss P. & Wagreich M. 2010: Lower Miocene structural evolution of the central Vienna Basin (Austria). *Mar. Petrol. Geol.* 27, 3, 666–681.

Kamptner E. 1948: Coccolithen aus dem Torton des Inneralpinen Wiener Beckens. *Sitz.-Ber. Österr. Akad. Wiss., Math.-Naturwiss. Kl.* 1, 157, 1–16.

Kázmér M. 1990: Birth, life and death of the Pannonian Lake. *Palaeogeogr. Palaeoclimatol. Palaeoecol.* 79, 1–2, 171–188.

Kilényi E. & Šefara J. 1989: Pre-Tertiary basement contour map of the Carpathian Basin beneath Austria, Czechoslovakia and Hungary. *Eötvös Lóránd Geophys. Inst.*, Budapest.

Kováč M., Baráth I., Kováčová-Slamková M., Pipík R., Hlavatý I. & Hudáčková N. 1998a: Late Miocene paleoenvironments and sequence stratigraphy: Northern Vienna Basin. *Geol. Carpathica* 49, 6, 445–458.

Kováč M., Nagymarosy A., Oszczypko N., Ślączka A., Csontos L., Marunteanu M., Matenco L. & Márton M. 1998b: Palinspastic reconstruction of the Carpathian-Pannonian region during the Miocene. In: Rakús M. (Ed.): Geodynamic development of the Western Carpathians. *Geol. Surv. Slovak Republic*, Bratislava, 189–217.

Kováč M., Baráth I., Harzhauser M., Hlavatý I. & Hudáčková N. 2004: Miocene depositional systems and sequence stratigraphy of the Vienna Basin. *Cour. Forsch.-Inst. Senckenberg* 246, 187–212.

Kováč M., Andreyeva-Grigorovich A., Bajraktarevic Z., Brzobohatý R., Filipescu S., Fodor L., Harzhauser M., Nagymarosy A., Oszczypko N., Pavelic D., Rögl F., Saftic B., Sliva L. & Studencka B. 2007: Badenian evolution of the Central Paratethys Sea: paleogeography, climate and eustatic sea-level changes. *Geol. Carpathica* 58, 6, 579–606.

Kováč M., Sliva L., Sopková B., Hlavatá J. & Škulová A. 2008: Serravallian sequence stratigraphy of the northern Vienna Basin: high frequency cycles in the Sarmatian sedimentary record. *Geol. Carpathica* 59, 6, 545–561.

Kreutzer N. 1974: Distribution of some sand- and gravel beds of the Sarmatian and uppermost Badenian in the Matzen area, Vienna Basin. *Erdoel-Erdgas-Z.* 90, 4, 114–127.

Kreutzer N. 1986: Die Ablagerungssequenzen der miozänen Badener Serie im Feld Matzen und im zentralen Wiener Becken. *Erdoel-Erdgas-Z.* 102, 492–503.

Kreutzer N. & Hlavatý V. 1990: Sediments of the Miocene (mainly Badenian) in the Matzen area in Austria and in the southern part of the Vienna Basin in Czechoslovakia. In: Minarikove D. & Lobitzer H. (Eds.): Thirty years of geological cooperation between Austria and Czechoslovakia. *UUG*, Praha, 110–123.

Krijgsman W. & Kent D.V. 2004: Non-uniform occurrence of short-term polarity fluctuations in the geomagnetic field? New results from Middle to Late Miocene sediments of the North Atlantic (DSDP Site 608): Geophysical monograph series. *AGU* 145, 328.

Lankreijer A., Kováč M., Cloetingh S., Pitoňák P., Hlôška M. & Biermann C. 1995: Quantitative subsidence analysis and forward modelling of the Vienna and Danube basins: thin-skinned versus thick-skinned extension. *Tectonophysics* 252, 1–4, 433–451.

Lirer F., Harzhauser M., Pelosi N., Piller W.E., Schmid H.P. & Sprovieri M. 2009: Astronomically forced teleconnection between Paratethyan and Mediterranean sediments during the Middle and Late Miocene. *Palaeogeogr. Palaeoclimatol. Palaeoecol.* 275, 1–4, 1–13.

Lourens L.J., Hilgen F.J., Laskar J., Shackleton N.J. & Wilson D. 2004: The Neogene Period. In: Gradstein F.M., Ogg J.G. & Smith A.G. (Eds.): A geological time scale 2004. *Cambridge University Press*, Cambridge, 409–440.

Luthi S.M. 2001: Geological well logs, their use in reservoir modelling. *Springer*, Berlin, 1–373.

Magyar I., Geary D.H. & Muller P. 1999: Paleogeographic evolution of the Late Miocene Lake Pannon in Central Europe. *Palaeogeogr. Palaeoclimatol. Palaeoecol.* 147, 3–4, 151–167.

Magyar I., Lantos M., Ujszaszi K. & Kordos L. 2007: Magnetostratigraphic, seismic and biostratigraphic correlations of the Upper Miocene sediments in the northwestern Pannonian Basin System. *Geol. Carpathica* 58, 3, 277–290.

Martini E. 1971: Standard Tertiary and Quaternary calcareous nannoplankton zonation. *Proceedings of the II Planktonic Conference. Ed. Tecnoscienza*, Roma, 739–785.

Miller K.G., Wright J.D. & Fairbanks R.G. 1991: Unlocking the ice house — Oligocene-Miocene oxygen isotopes, eustasy, and margin erosion. *J. Geophys. Res., Solid Earth and Planets* 96, B4, 6829–6848.

Papp A. 1951: Das Pannon des Wiener Beckens. *Mitt. Geol. Gesell., Wien* 39–41, 99–193.

Papp A. 1974: Boundary stratotypus: Bohrung Niedersulz No. 3, 5, 9. Wiener Becken, Österreich. In: Papp A., Marinescu F. & Seneš J. (Eds.): M5. Sarmatien (sensu E. Suess 1866). Chronostratigraphie und Neostratotypen. *Verlag der Slowakischen Akademie der Wissenschaften 4*, Bratislava, 318–427.

Papp A. & Schmid M. 1985: Die fossilen Foraminiferen des tertiären Beckens von Wien. *Abh. Geol. Bundesanst.* 37, 1–311.

Papp A., Cicha I. & Čtyroká J. 1978: Allgemeine Charakteristik der Foraminiferenfauna im Badenien. In: Papp A., Cicha I., Seneš J. & Steininger F.F. (Eds.): M4 — Badenien (Moravien, Wielicien, Kosovien). Chronostratigraphie und Neostratotypen. *Verlag der Slowakischen Akademie der Wissenschaften 4*, Bratislava, 263–268.

Peresson H. & Decker K. 1997: The Tertiary dynamics of the northern eastern alps (Austria): Changing palaeostresses in a collisional plate boundary. *Tectonophysics* 272, 2–4, 125–157.

Peresson M., Ćorić S. & Wimmer-Frey I. 2005: New stratigraphic and mineralogical data of Neogene sediments from the City of Vienna (Vienna Basin). *12th Congress R.C.M.N.S.,* 6–11 September 2005, Vienna, 176–177.

Piller W.E., Harzhauser M. & Mandic O. 2007: Miocene Central Paratethys stratigraphy — current status and future directions. *Stratigraphy* 4, 2–3, 151–168.

Pozzi J.P., Barthes V., Thibal J., Pocachard J., Lim M., Thomas T. & Pages G. 1993: Downhole magnetostratigraphy in sediments — comparison with the paleomagnetism of a core. *J. Geophys. Res., Solid Earth* 98, B5, 7939–7957.

Ratschbacher L., Frisch W., Linzer H.G. & Merle O. 1991: Lateral extrusion in the Eastern Alps. 2. Structural-analysis. *Tectonics* 10, 2, 257–271.

Riegl B. & Piller W.E. 2000: Biostromal coral facies — A Miocene example from the Leitha Limestone (Austria) and its actualistic interpretation. *Palaios* 15, 399–413.

Rögl F. 1998: Palaeogeographic considerations for Mediterranean and Paratethys Seaways (Oligocene to Miocene). *Ann. Naturhist. Mus., Wien* 99A, 279–310.

Sauer R., Seifert P. & Wessely G. 1992: Guidebook to excursions in the Vienna Basin and adjacent Alpine-Carpathian thrustbelt in Austria. *Mitt. Österr. Geol. Gesell.* 85, 5–96.

Scholger R. & Stingl K. 2004: New paleomagnetic results from the Middle Miocene (Karpatian and Badenian) in Northern Austria. *Geol. Carpathica* 55, 2, 199–206.

Schütz K., Harzhauser M., Rögl F., Čorič S. & Galović I. 2007: Foraminiferen und Phytoplankton aus dem unteren Sarmatium des südlichen Wiener Beckens (Petronell, Niederösterreich). *Jb. Geol. Bundesanst.* 147, 1–2, 449–488.

Seifert P. 1992: Palinspastic reconstruction of the easternmost Alps between upper Eocene and Miocene. *Geol. Carpathica* 43, 6, 327–331.

Seifert P. 1996: Sedimentary-tectonic development and Austrian hydrocarbon potential of the Vienna Basin. In: Wessely G. & Liebl W. (Eds.): Oil and gas in in Alpidic thurstbelts and basins of Central and Eastern Europe. *EAGE Spec. Publ.* 5, 331–341.

Sen A., Kendall C.G.S. & Levine P. 1999: Combining a computer simulation and eustatic events to date seismic sequence boundaries: a case study of the Neogene of the Bahamas. *Sed. Geol.* 125, 1–2, 47–59.

Steininger F.F. & Rögl F. 1985: Die Paläeogeographie der Zentralen Paratethys in Pannonien. In: Papp A., Jámbor Á. & Steininger F.F. (Eds.): Chronostratigraphie und Neostratotypen, Miozän der Zentralen Paratethys VII, M6, Pannonien. *Akadémiai Kiadó*, Budapest, 46–50.

Steininger F.F. & Wessely G. 2000: From the Tethyan Ocean to the Paratethys Sea: Oligocene to Neogene stratigraphy, paleogeography and paleobiogeography of the circum-Mediterranean region and the Oligocene to Neogene Basin evolution in Austria. *Mitt. Österr. Geol. Gesell.* 92, 95–116.

Stradner H. & Fuchs R. 1978: Das Nannoplankton in Österreich. In: Brestenská E. (Ed.): M4 Badenien (Moravien, Wielicien, Kosovien). Chronostratigraphie und Neostratotypen Miozän der Zentralen Paratethys. *VEDA*, *SAV*, Bratislava 6, 489–532.

Strauss P., Harzhauser M., Hinsch R. & Wagreich M. 2006: Sequence stratigraphy in a classic pull-apart basin (Neogene, Vienna Basin). A 3D seismic based integrated approach. *Geol. Carpathica* 57, 3, 185–197.

Thibal J., Etchecopar A., Pozzi J.P., Barthes V. & Pocachard J. 1999: Comparison of magnetic and gamma ray logging for correlations in chronology and lithology: example from the Aquitanian Basin (France). *Geophys. J. Int.* 137, 3, 839–846.

Turco E., Hilgen F.J., Lourens L.J., Shackleton N.J. & Zachariasse W.J. 2001: Punctuated evolution of global climate cooling during the late Middle to early Late Miocene: High-resolution planktonic foraminiferal and oxygen isotope records from the Mediterranean. *Paleoceanography* 16, 4, 405–423.

Vojtko R., Hók J., Kováč M., Sliva L., Joniak P. & Šujan M. 2008: Pliocene to Quaternary stress field change in the western part of the Central Western Carpathians (Slovakia). *Geol. Quart.* 52, 1, 19–30.

Wagreich M. & Schmid H.P. 2002: Backstripping dip-slip fault histories: apparent slip rates for the Miocene of the Vienna Basin. *Terra Nova* 14, 3, 163–168.

Weissenbäck M. 1996: Lower to Middle Miocene sedimentation model of the central Vienna Basin. In: Wessely G. & Liebl W. (Eds.): Oil and gas in Alpidic thurstbelts and basins of Central and Eastern Europe. *EAGE Spec. Publ.* 5, 355–363.

Wessely G. 1988: Structure and development of the Vienna Basin in Austria. In: Royden L. & Horvath F. (Eds.): The Pannonian Basin. A study in basin evolution. *AAPG Mem.* 45, 333–346.

Wessely G. 2000: Sedimente des Wiener Beckens und seiner alpinen und subalpinen Unterlagerung. *Mitt. Gesell. Geol. Bergbaustud. Österr.* 44, 191–214.

Westerhold T., Bickert T. & Röhl U. 2005: Middle to late Miocene oxygen isotope stratigraphy of ODP site 1085 (SE Atlantic): new constrains on Miocene climate variability and sea-level fluctuations. *Palaeogeogr. Palaeoclimatol. Palaeoecol.* 217, 3–4, 205–222.

Willenbring J.K. & Blanckenburg F.v. 2010: Long-term stability of global erosion rates and weathering during late-Cenozoic cooling. *Nature* 465, 13, 211–214.

Williams T. 2006: Magnetostratigraphy from downhole measurements in ODP holes. *Physics Earth Planet. Interiors* 156, 3–4, 261–273.